# Thermal and Flow Phenomena in a Reacting Magneto-Nanofluid over an Exponentially Expanding Sheet with a Non-Equilibrium Heat Source

## Abstract

The current study examines the flow and heat transmission mechanism of magneto-nanofluid over an exponentially stretching plate under the influence of varying heat source and activation energy. The motion is driven by the exponentially stretching sheet and subjected to a transverse magnetic field, and variable heat source of space-and temperature-dependent form. The concentration field models activation energy effects alongside chemical reaction kinetics, capturing the behaviour of reactive nanofluid systems. The current problem is developed using relevant laws to generate partial differential equations and transformed into ordinary differential equations by similarity variables and then numerically solved using the Runge–Kutta–Fehlberg method coupled with a shooting technique. Results indicate that there is a suppression of the hydrodynamic bounding surface due to higher magnetic influence but the thermal field enlarges as the heat source intensifies while the concentration field enhances with escalating values of the activation energy. These results can be applied in various engineering and industrial applications, such as found in polymer and plastic manufacturing, catalytic chemical reactors, and electronic device cooling.

**Keywords:** Exponentially stretching sheet; variable heat source; magnetohydromagnetic, Reactive-Radiative fluid.

## Introduction

Magneto-nanofluids describe the interaction between magnetic fields and electrically conducting nanofluids. They consist of magnetic nanoparticles suspended in conventional heat transfer fluids, enabling the fluid to respond to external magnetic fields while exhibiting enhanced thermal conductivity. Their superior ability to transfer heat, combined with tunable rheological properties, makes them particularly valuable in advanced engineering systems (Ali, et al., 2020; Raju et al., 2016; Fatunmbi et al., 2021; Ahmed et al., 2023). Unlike traditional fluids, magneto-nanofluids offer precise control over flow behavior and temperature distribution via magnetic field manipulation, leading to significant improvements in thermal system performance. These unique characteristics have led to a wide range of engineering and industrial applications. In nuclear reactors, magneto-nanofluids serve as efficient coolants that help reduce thermal hotspots and improve operational safety. In solar thermal systems, they enhance heat absorption and storage capabilities, contributing to better energy conversion efficiency (Tshivhi, K. S., & Makinde, 2021; Zeeshan et al., 2021, Akbar et al., 2021). The automotive and aerospace sectors employ them in high-performance cooling systems for engines and avionics. Additionally, they are increasingly used in electronic cooling applications, where managing heat in compact, high-power devices is critical. These various applications have encouraged many scholars to study this concept (see Khan et al., 2018, Eld et al., 2018; Zhang et al., 2023) on diverse geometries for both Newtonian and non-Newtonian fluids.

Radiative heat transfer plays a central character in the study of fluid dynamics, especially in high-temperature environments where it applies a substantial influence on the transmission of heat energy (Fatunmbi & Adeniyan, 2020; Jalili et al, 2023). Likewise, in many engineering and industrial systems, the presence of a non-uniform heat source or sink significantly affects thermal transport characteristics. Unlike idealized uniform heating, non-uniform heat sources reflect realistic thermal gradients arising from internal heat generation, radiation effects, or spatially varying thermal loads. These conditions are commonly encountered in nuclear reactors, electronic devices, combustion chambers, and solar thermal collectors, where temperature-dependent heat generation impacts system efficiency and stability. Thus, Thumma et al, (2022) investigated a 3D flow dynamic of nanofluid subject to non-uniform heat source passing through an expanding sheet whereas, Abel& Nandeppanavar (2009) considered such a concept when studying heat transport of a hydromagnetic viscoelastic fluid over a stretching device while Fatunmbi & Salawu (2020) explore such a concept on magneto-micropolar fluid experiencing nonlinear velocity and entropy generation.

Simultaneously, the inclusion of a chemical reaction within the flow adds complexity, especially in reacting fluid systems where heat and mass transfer are coupled. Chemical reactions may be endothermic or exothermic, influencing the temperature field and flow behavior. This is particularly relevant in polymer processing, catalytic reactors, and biochemical systems, where controlling reaction rates is essential for desired product yields. Furthermore, the concept of activation energy—the minimum energy required for a chemical reaction to occur—plays a pivotal role in determining the reaction rate. Incorporating activation energy into heat and mass transfer models allows for a more accurate depiction of reaction kinetics, especially in high-temperature combustion, fuel cells, and nanofluid-based chemical reactors, where energy barriers critically govern performance. For these reasons, Hamid & Khan (2018) considered the simultaneous impacts of binary chemical reaction and activation energy on a transient motion of magneto-non-Newtonian Williamson fluid consisting of nanoparticles. In another study, Khan and Alzahrani (2020) evaluated such a combined influence on the flow motion of a non-Newtonian fluid in the presence of nanoparticles. Fatunmbi et al. (2023) assessed the transport phenomenon of a reactive Tangent-hyperbolic fluid subject to nonlinear mixed convection, and activation energy. Other relevant facts about these concepts and their applications can be found in Mustapha et al. (2017); Javeed et al. (2019) and Khan et al. (2020). However, none of these studies have been conducted on an exponentially expanding sheet in spite of such useful applications derivable from it.

The aim of the present study is to develop a mathematical model that captures the coupled nonlinear partial differential equations governing the thermal and flow dynamics of a magneto-nanofluid over an exponentially expanding porous sheet. The model accounts for critical physical effects such as chemical reaction, thermal radiation, activation energy, and the influence of a non-equilibrium heat source, thereby reflecting realistic and complex transport phenomena. By applying appropriate similarity transformations, the governing equations are reduced to a system of ordinary differential equations, which are then solved numerically using a combination of the shooting method and the Runge-Kutta-Fehlberg scheme. The numerical results show excellent agreement with previously published studies, thereby confirming the reliability and accuracy of

the proposed methodology. The application of this study can be found in a variety of engineering and technological fields, particularly in aerospace systems, jet propulsion mechanisms, and space dynamics, where enhanced thermal and fluid control is crucial.

## 1. Problem Development and Formulation

In this section, the assumptions for the formulation of the governing equations are outlined, followed by the derivation of the descriptive equations for the transport phenomena. The following assumptions are put in place:

- The nanofluid flow is incompressible and steady.
- A constant magnetic field of strength $B_0$ is applied externally normal to the flow routes.
- The flow occurs over a two-dimensional exponentially porous stretching sheet, with the sheet velocity defined as $u = U_w(X) = U_0K$.
- The flow route is along the $x$-direction, while the $y$-direction is perpendicular to it as illustrated in Figure 1.
- There is a mass flux at the surface, characterized by a suction/injection velocity $v = S_0(X) = -S_0H$.
- The surface temperature and nanoparticle concentration at the sheet are maintained at $E_w$ and $N_w$ respectively.
- The energy equation accounts for both space and temperature-dependent heat source/sink $Nh$, thermophoretic diffusion, Brownian motion, and viscous dissipation as expressed in equation (3), while chemical reaction and activation energy. Are added in the concentration region.

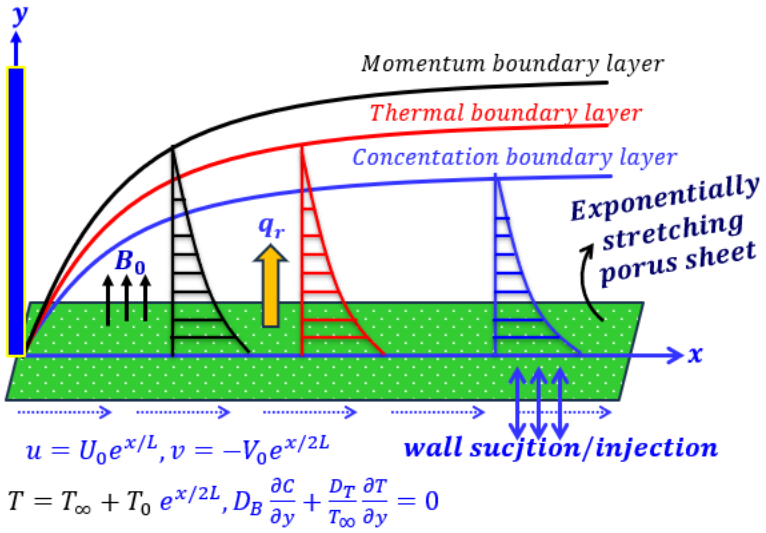


**Figure 1**. Schematic diagram of flow configuration

Taking cognizance of the aforementioned assumptions and using the prominent boundary layer assumptions, the appropriate equations controlling the transport phenomena are:

$$\frac{\partial U}{\partial X} + \frac{\partial V}{\partial Y} = 0, \tag{1}$$

$$\rho_f\left(u\frac{\partial U}{\partial X}+v\frac{\partial U}{\partial Y}\right)=\mu_f\frac{\partial^2 U}{\partial Y^2}-\sigma B_o^2U-\frac{\mu_f}{\kappa p}U+\frac{Fs}{\kappa p}U^2 \quad (2)$$

$$\rho_f Cp\left(u\frac{\partial E}{\partial X}+v\frac{\partial E}{\partial Y}\right)=k_f\frac{\partial^2 E}{\partial y^2}-\frac{\partial q_r}{\partial Y}+\mu_f\left(\frac{\partial u}{\partial y}\right)^2+\tau\left\{D_B\frac{\partial N}{\partial Y}\frac{\partial E}{\partial Y}+\frac{D_T}{T_\infty}\left(\frac{\partial E}{\partial Y}\right)^2\right\}+Nh\Big\}, \quad (3)$$

$$u\frac{\partial N}{\partial X}+v\frac{\partial N}{\partial Y}=Db\frac{\partial^2 N}{\partial Y^2}+\frac{D_T}{T_\infty}\frac{\partial^2 T}{\partial Y^2}-\gamma(N-N_\infty)^2\left(\frac{T}{T_\infty}\right)^m e^{\frac{E_a}{kT}}, \quad (4)$$

Equations (1-3) are subject to the boundary condition as

$$U=U_w(X)=U_0K,\ v=-S(X)=-S_0H, E=E_w=E_\infty+E_0H, D_B\frac{\partial N}{\partial Y}+\frac{D_t}{E_\infty}\frac{\partial E}{\partial Y}=0\ \ at\ Y=0$$
$$U\to 0,\quad E\to E_\infty,\quad C\to C_\infty,\ as\ Y\to\infty. \quad (5)$$

Where $K=e^{\frac{X}{L}}$ and $H=e^{\frac{X}{2L}}$. The term $Nh$ in the energy equation (2) represents the non-uniform heat source of space and thermal-dependent heat source. This $Nh$ is expressed as

$$Nh=-\frac{k\,U_w}{X\,\vartheta}\{L^*(E_w-E_\infty)f'+J^*(E-E_\infty)\} \quad (6)$$

**Similarity Transformation Quantities**

The similarity variables in equation (7) are introduced for the conversion of the partial differential equations modelling the problem.

$$U=U_0\,Kf'(\xi),\quad V=-\sqrt{\frac{\vartheta U_0}{2L}}e^{\frac{X}{2L}}\left(f(\xi)+\eta f'(\xi)\right),\qquad E=E_\infty+E_0\,H\,\theta(\xi),$$
$$N=N_w=N_\infty+N_0\,\phi(\xi),\quad \xi=Y\sqrt{\frac{U_0}{2\,\vartheta\,L}}e^{\frac{X}{2L}} \quad (7)$$

On implementing (6), the mass conservation (1) becomes valid while equations (2-4) transformed to the underlisted nonlinear ordinary derivatives listed in equations (9-11).

$$\frac{d^3f}{d\xi^3}+f(\xi)\frac{d^2f}{d\xi^2}-\left(\frac{df}{d\xi}\right)^2-\frac{df}{d\xi}(M+K)=0, \quad (8)$$

$$(1+R)\frac{d^2\theta}{d\theta^2}+\Pr\left[Ec\left(\frac{d^2f}{d\xi^2}\right)^2+Nb\frac{d\theta}{d\xi}\frac{d\phi}{d\xi}+Nt\left(\frac{d\theta}{d\xi}\right)^2+f(\xi)\frac{d\theta}{d\xi}-\frac{df}{d\xi}\theta(\xi)\right]+(A^*\frac{df}{d\xi}+$$
$$B^*\theta(\xi))=0 \quad (9)$$

$$\frac{d^2\phi}{d\theta^2}+Sc\left(f\frac{d\phi}{d\xi}-\frac{df}{d\xi}\phi\right)+\frac{Nt}{Nb}\frac{d^2\theta}{d\theta^2}+Sc\ Cr\phi(\xi)(1+\delta\theta(\xi))^n exp^{\left(\frac{E}{1+\delta\theta(\xi)}\right)}=0 \quad (10)$$

These equations are subject to:

$$\left.\begin{aligned} f(0)=S_w,\quad \frac{df}{d\xi}(0)=1,\quad \theta(0)=1,\quad \frac{d\phi}{d\xi}(0)=-\frac{Nt}{Nb}\frac{d\theta}{d\xi}(0)\qquad at\ \xi=0,\\ \frac{df}{d\xi}(\xi)\to 0,\qquad \theta(\xi)\to 0,\qquad \phi(\xi)\to 0\qquad as\ \xi\to\infty \end{aligned}\right\} \quad (11)$$

Where $S_w<0$ $(S_w>)$ represents injection (suction). The terms featured as parameters are : $M, K, Pr, R, Nb, Nt, Sc, Ec, Cr, \delta,$ and $E$ named as a magnetic intensity, porosity factor, Prandtl number, radiation factor, Brownian motion term, thermophoresis term, Schmidt number, Eckert number, reaction rate, heat relative term, and energy activation term respectively. The description of these terms is:

$$\left.\begin{aligned} M=\frac{2\sigma B_0^2 l}{\rho\,U_w},\ K=\frac{2\nu l}{k_p^*U_w},\ Pr=\frac{\nu\rho c_p}{k},\ R=\frac{16\,\sigma^*T_\infty^3}{3\,k\,k^*},\ Nb=\frac{\tau\,D_B\,(C_w-C_\infty)}{\upsilon},\ Nt=\frac{D_T\,(T_w-T_\infty)}{T_\infty\upsilon},\\ Sc=\frac{\nu_f}{D_B}, Ec=\frac{U_w^2}{c_p\,(T_w-T_\infty)},\ Cr=\frac{2k_r^2}{U_w},\ \delta=\frac{T-T_\infty}{T_\infty},\quad E=\frac{-E_a}{kT_\infty}, \end{aligned}\right\} \quad (12)$$

The useful terms for the engineering society include the surface drag, thermal gradient and mass concentration gradient. These are sequentially indicated as:

$$Cf_x = \frac{2\tau_w}{\rho\, U_w^2}, \quad Nu_x = \frac{xq_w}{k(T_w - T_\infty)}, \quad Sh_x = \frac{xq_m}{D_B(C_w - C_\infty)} \tag{13}$$

Where $\tau_w = \mu \left.\frac{\partial u}{\partial y}\right|_{y=0}$ is the wall drag force, $q_w = -k\left(1 + \frac{16\sigma^* T_\infty^3}{3k\,k^*}\right)\left.\frac{\partial T}{\partial y}\right|_{y=0}$, is the wall heat flux, and $q_m = -D_B \left.\frac{\partial T}{\partial y}\right|_{y=0}$ The dimensionless quantities are expressed as

$$z\sqrt{Re_x}Cf_x = 2\,f''(0), \frac{2}{\sqrt{Re_x}}\,Nu_x = -(1+R)\,\theta'(0), \frac{2}{\sqrt{Re_x}}\,Sh_x = -\phi'(0) \tag{14}$$

## 2. Method of Solution and Validation of Results

The set of equations (8-11) constitutes a nonlinear boundary value problem which is solved numerically due to its highly nonlinearity. A numerical technique through shooting procedure is employed along with the Rung-Kutta Felherb scheme to solve the problem. The code for the equations is written and a symbolic Maple algebra software is engaged for the computations. The obtained results are validated by comparison with previous results under limiting scenarios and found to be in excellent agreement as recorded in Table 1. The numerical study is done with the default values listed as $M = 0.5, K = 0.7, R = 0.3, A = 0.3, B = 0.7, Ec = 0.3, Nt = 0.5, Nb = 0.5, Sc = 0.4, \delta = 0.35, E = 0.07, f_w = 0.2, n = 1.0$ and $Cr = 0.06$ as obtained from relevant existing studies in the literature.

**Table 1:** Computations of the heat transfer physical phenomenon for various values of $Pr$ as compared with existing results

| $Pr$ | Aziz and Afify (2019) | Abolbashari et al. (2015) | The results for the current study |
|---|---|---|---|
| 0.20 | 0.1691 | 0.1691 | 0.16907329 |
| 0.70 | 0.4538 | 0.4539 | 0.45388105 |
| 2.00 | 0.9113 | 0.9114 | 0.91136973 |
| 7.00 | 1.8954 | 1.8954 | 1.89535789 |

## 3. Results and Discussion

A boundary value model is developed and invariantly transformed to theoretically analyze the thermofluidic properties and parametric sensitivities of the fluid flow thermal and species distributions in a horizontal porous device. To further understand the flow phenomena, various graphs are included on the dimensionless profiles and discussed under this section.

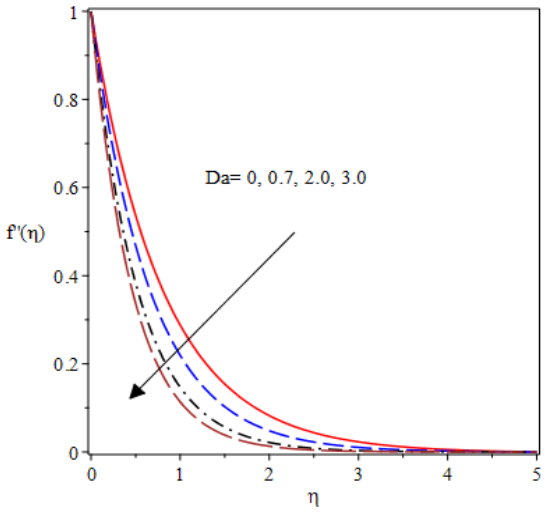


**Fig. 2.** Velocity profiles for various values of $Da$

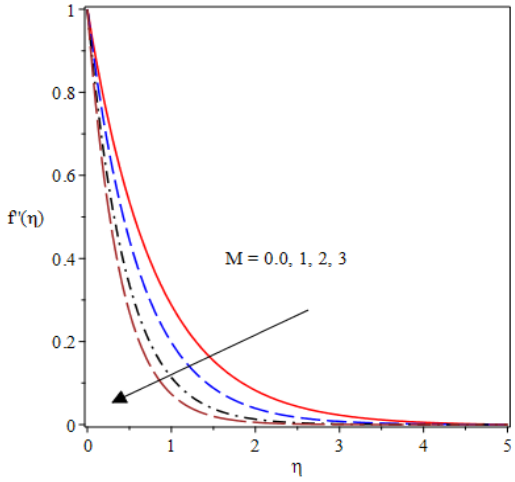


**Fig. 3.** Velocity profiles for various values of $M$

The velocity has a decline trend as the Darcy permeability factor raised, as illustrated in Fig. 2. In essence, as the Darcy permeability factor rises, the fluid's velocity decelerates due to resisting forces due to high permeability. The Fig. 3 illustrates a decline in flow rate for a higher magnetic term. Enhancing the magnetic field vitality generally enables the velocity, owing to the enhanced Lorentz force opposing the flow. When a magnetic field engages a conducting nanofluid, Lorentz forces are generated, which in turn can either speed up or slow down the flowing fluid, reliant on the magnetic field's strength and direction. Introducing a magnetic field into a conducting fluid applies a force on the charge-carrying particles within the fluid. The force is called Lorentz force and is normal to the magnetic field axis and the fluid flow direction. The Lorentz force resists fluid flow motion and hinders its flow. This suppression occurs because the magnetic field exerts a Lorentz force that resists the liquid's motion. This reduction in surface area leads to lower surface resistance, thereby enhancing the velocity.

Fig. 4 and 5 highlight the effect of heat source factor $A$ on temperature. And concentration profiles. As noticed, this results in a rise in the fluid temperature due to the accumulation of heat generated inside the floe domain. This additional energy raises the fluid's temperature, leading to a more noticeable thermal gradient. The results in Fig. 6 and 7 display how the value $B$ affects dimensionless temperature $\theta(\eta)$. And concentration $(\phi(\eta)$.It is revealed that temperature distribution rises for greater $B$ values. The nanoparticle heat propagation is prompted as the fluid particles collide and random motion is propelled along the far stream thereby encouraging

temperature distribution. When more thermal energy is undertaken in the nanofluid system, the heat source component distributes temperature better.

**Fig4.** Thermal field distribution for various $A$ **Fig. 5.** Concentration profiles for various $A$

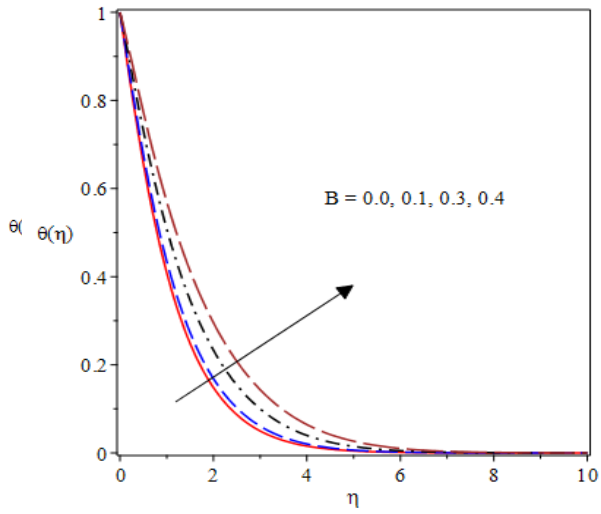


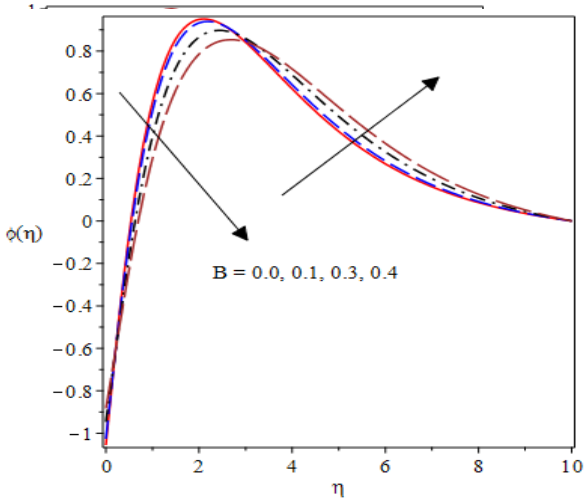


**Fig 6.** Concentration profiles for various $Sc$ **Fig. 7.** Concentration profiles for various $\epsilon$

Fig. 8 investigates the mass concentration behavior for increasing values of the Schmidt number. It is demonstrated that the concentration field reduces as the Schmidt quantity increases. This is brought about by the opposing relationship between mass diffusivity and the Schmidt value. It demonstrates a decrease in concentration as the Schmidth number rises, a rise in Schmidth implies more momentum transfer than mass transfer. Fig. 9, explains that the concentration $\phi(\eta)$ reduces with a boost in the species reaction $Cr$ term because a stronger reaction rate leads to faster consumption of the species. This depletion outpaces replenishment by diffusion or convection, leading to a net declination in $\phi(\eta)$ throughout the fluid domain.

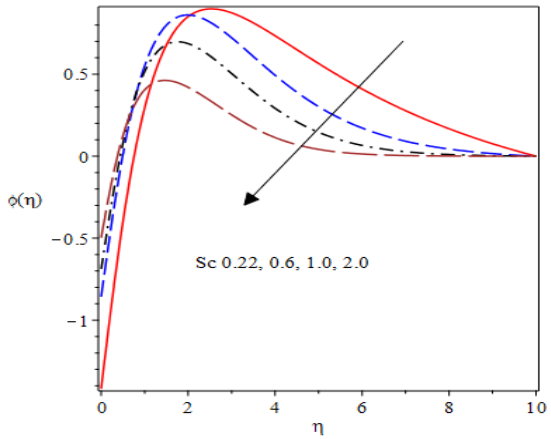


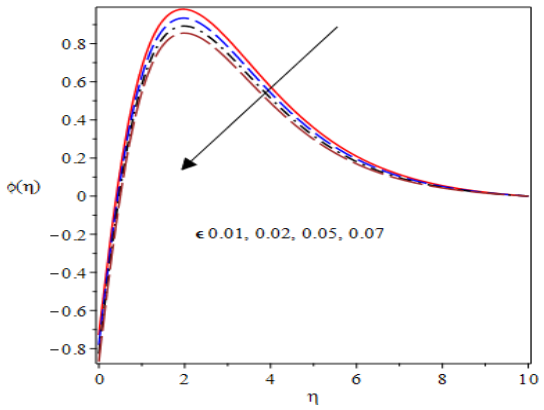


**Fig 8.** Concentration profiles for various $Sc$ **Fig.9.** Concentration profiles for various $Cr$

The effect of the temperature-relative parameter is presented in Fig. 10, which shows a decrease with the increase in its value. When the positive turning of the species reaction rate term makes the nanoparticle and the surrounding fluid react at a faster rate. An increase in the activation energy term $E$ caused the nanoparticles concentration profiles to rise as depicted in Figure 11.

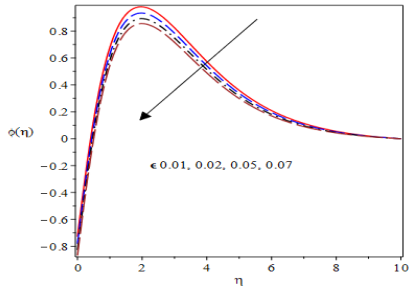


**Fig 10.** Concentration profiles for various $a$

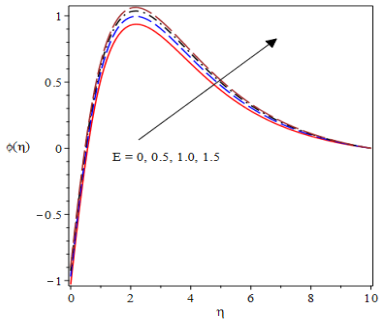


**Fig.11.** Concentration profiles for various $E$

## Conclusion

This research looks at the radiative-free convection flow of a magnetic nanomaterial past a permeable exponential stretchy plate, which produces an uneven internal heat generation. A perpendicular magnetic field influences the nanofluid flow. The impacts of activation energy are explored. The partial derivative model is converted into ordinary derivative equations by adjusting multi-class parameters using a modified partitioning weighted residual scheme in the MAPLE package. The Galerkin technique is employed iteratively to determine various parameter values, with all computations carried out in the Maple software environment to ensure accuracy. The outputs are displayed in plots and tables, demonstrating the impacts of diverse fluid terms. Statistics show that these features have a considerable impact on flow properties, as well as heat and species transport rates. The findings are described below, as follows;

- Increasing magnetic and porosity terms leads to a reduction in flow velocity, signifying a retarding tendency.
- The Buongiorno model of nanofluid has been effectively utilized to examine how nanoparticle concentration affects the diffusivity of nanofluids.
- To justify non-Newtonian fluid behaviors, the study effortlessly combines generalized fluxes for the transport of heat and species in a nanofluid.
- Activation energy term boosts the concentration profiles whereas the temperature relative term caused a decrease in the concentration profiles.
- The thermal boundary layer structure thickens for both space-dependent and temperature dependent heat source.
- The mass transfer rate was observed to elevate by improving the energy activation term.

This research investigation helps to understand and optimize the behavior of complex systems with significant microstructural and rotational impacts. Their uses are many, ranging from healthcare to energy, industry, and environmental engineering, making them essential components of modern scientific and industrial achievements.

## References

Abel, M. S., & Nandeppanavar, M. M. (2009). Heat transfer in MHD viscoelastic boundary layer flow over a stretching sheet with non-uniform heat source/sink. *Communications in Nonlinear Science and Numerical Simulation*, *14*(5), 2120-2131.

Ahmed, N., Khan, U., & Mohyud-Din, S. T. (2018). Influence of shape factor on flow of magneto-nanofluid squeezed between parallel disks. *Alexandria engineering journal*, *57*(3), 1893-1903.

Akbar, N. S., Bég, O. A., & Khan, Z. H. (2017). Magneto-nanofluid flow with heat transfer past a stretching surface for the new heat flux model using numerical approach. *International Journal of Numerical Methods for Heat & Fluid Flow*, *27*(6), 1215-1230.

Ali, M., Sultan, F., Khan, W. A., Shahzad, M., & Arif, H. (2020). Important features of expanding/contracting cylinder for Cross magneto-nanofluid flow. *Chaos, Solitons & Fractals*, *133*, 109656.

Eid, M. R., & Makinde, O. D. (2018). Solar radiation effect on a magneto nanofluid flow in a porous medium with chemically reactive species. *International Journal of Chemical Reactor Engineering*, *16*(9), 20170212.

Fatunmbi, E. O., & Adeniyan, A. (2020). Nonlinear thermal radiation and entropy generation on steady flow of magneto-micropolar fluid passing a stretchable sheet with variable properties. *Results in Engineering*, *6*, 100142.

Fatunmbi, E. O., & Salawu, S. O. (2020). Thermodynamic second law analysis of magneto-micropolar fluid flow past nonlinear porous media with non-uniform heat source. *Propulsion and Power Research*, *9*(3), 281-288.

Fatunmbi, E. O., Adigun, A. J., & Salawu, S. O. (2023). Dual stratification mechanism for nonlinear mixed convective magneto-tangent hyperbolic fluid over a stretchable device with activation energy. *International Journal of Applied and Computational Mathematics*, *9*(4), 48.

Fatunmbi, E. O., Ramonu, O. J., & Salawu, S. O. (2023). Analysis of heat transfer phenomenon in hydromagnetic micropolar nanoliquid over a vertical stretching material featuring convective and isothermal heating conditions. *Waves in Random and Complex Media*, 1-20.

Hamid, A., & Khan, M. (2018). Impacts of binary chemical reaction with activation energy on unsteady flow of magneto-Williamson nanofluid. *Journal of Molecular Liquids*, *262*, 435-442.

Jalili, P., Azar, A. A., Jalili, B., & Ganji, D. D. (2023). Study of nonlinear radiative heat transfer with magnetic field for non-Newtonian Casson fluid flow in a porous medium. *Results in Physics*, *48*, 106371.

Javed, M., Alderremy, A. A., Farooq, M., Anjum, A., Ahmad, S., & Malik, M. Y. (2019). Analysis of activation energy and melting heat transfer in MHD flow with chemical reaction. *The European Physical Journal Plus*, *134*(6), 256.

Khan, M. I., & Alzahrani, F. (2020). Binary chemical reaction with activation energy in dissipative flow of non-Newtonian nanomaterial. *Journal of Theoretical and Computational Chemistry*, *19*(03), 2040006.

Khan, M., Ahmad, L., & Gulzar, M. M. (2018). Unsteady Sisko magneto-nanofluid flow with heat absorption and temperature dependent thermal conductivity: a 3D numerical study. *Results in Physics*, *8*, 1092-1103.

Khan, N. S., Kumam, P., & Thounthong, P. (2020). Second law analysis with effects of Arrhenius activation energy and binary chemical reaction on nanofluid flow. *Scientific reports*, *10*(1), 1226.

Mustafa, M., Khan, J. A., Hayat, T., & Alsaedi, A. (2017). Buoyancy effects on the MHD nanofluid flow past a vertical surface with chemical reaction and activation energy. *International Journal of Heat and Mass Transfer*, *108*, 1340-1346.

Raju, C. S. K., Sandeep, N., & Sugunamma, V. (2016). Unsteady magneto-nanofluid flow caused by a rotating cone with temperature dependent viscosity: a surgical implant application. *Journal of Molecular Liquids*, *222*, 1183-1191.

Thumma, T., Mishra, S. R., Abbas, M. A., Bhatti, M. M., & Abdelsalam, S. I. (2022). Three-dimensional nanofluid stirring with non-uniform heat source/sink through an elongated sheet. *Applied Mathematics and Computation*, *421*, 126927.

Tshivhi, K. S., & Makinde, O. D. (2021). Magneto-nanofluid coolants past heated shrinking/stretching surfaces: dual solutions and stability analysis. *Results in Engineering*, *10*, 100229.

Zeeshan, A., Pervaiz, Z., Shehzad, N., Nayak, M. K., & Al-Sulami, H. H. (2021). Optimal thermal performance of magneto-nanofluid flow in expanding/contracting channel. *Journal of Thermal Analysis and Calorimetry*, *143*, 2189-2201.

Zhang, X., Yang, D., Katbar, N. M., Jamshed, W., Ullah, I., Eid, M. R., ... & El Din, S. M. (2023). Entropy and thermal case description of monophase magneto nanofluid with thermal jump and Ohmic heating employing finite element methodology. *Case Studies in Thermal Engineering*, *45*, 102919.